Observing Axion Emission from Supernova with Collider Detectors

Based on

S. Asai (Tokyo U., ICEPP), YK, T. Moroi (Tokyo U.) and T. Sichanugrist (Tokyo U.),

arXiv:2203.01519 [hep-ph], Phys. Lett. B 829 (2022) 137137.

Yoshiki Kanazawa   Tokyo U. D2

ECFA HF WG1: 1st Workshop of the WG1-SRCH group, 25 May, 2022

My previous work

Supernova-scope for the direct search of Supernova axions

Shao-Feng Ge,[a,b,c] Koichi Hamaguchi,[d,e] Koichi Ichimura,[f,e]
Koji Ishidoshiro,[f] Yoshiki Kanazawa,[d] Yasuhiro Kishimoto,[f,e]
Natsumi Nagata[d] and Jiaming Zheng[a,b]

JCAP 11 (2020) 059

Supernova axion search with helioscope

Introduction

Axions

QCD Axion — solution to the strong CP problem

S. Weinberg, Phys. Rev. Lett. 40 (1978) 223;
F. Wilczek, Phys. Rev. Lett. 40 (1978) 279.

Axion-like particles (ALPs) — predicted in the string theories

P. Svrcek and E. Witten, JHEP 06 (2006) 051;
A. Arvanitaki, S. Dimopoulos and S. Dubovsky, Phys. Rev. D 81 (2010) 123530.

Axions are well-motivated candidates for the BSM.

But, they have not been found directly.

Constraints on axion models

Effective lagrangian at low energy

$$\mathscr{L} = \mathscr{L}_{SM} + \frac{1}{2}(\partial_\mu a)^2 + \frac{1}{2} m_a^2 a^2 + \frac{1}{4} g_{a\gamma\gamma} a F^{\mu\nu} \widetilde{F}_{\mu\nu} + \sum_{N=p,n} \frac{g_{aNN}}{2m_N} \overline{N} \gamma^\mu \gamma^5 N \partial_\mu a$$

m_a axion mass

$g_{a\gamma\gamma}$ axion-photon coupling

g_{aNN} axion-nucleon coupling

Constraints

$g_{a\gamma\gamma} \lesssim 6.6 \times 10^{-11}\ \mathrm{GeV}^{-1}$ for $m_a \lesssim 0.02\ \mathrm{eV}$ from CAST experiment

CAST collaboration, Nature Phys. 13 (2017) 584.

$\widetilde{g}_{aNN} \lesssim 6.4 \times 10^{-10}$ from SN 1987A $\widetilde{g}^2_{aNN} \equiv g^2_{ann} + 0.61 g^2_{app} + 0.53 g_{ann} g_{app}$

P. Carenza, T. Fischer et al., JCAP 10 (2019) 016.

Supernova

Supernova

- Red- or blue-supergiant
- $M \gtrsim 10\ M_\odot$

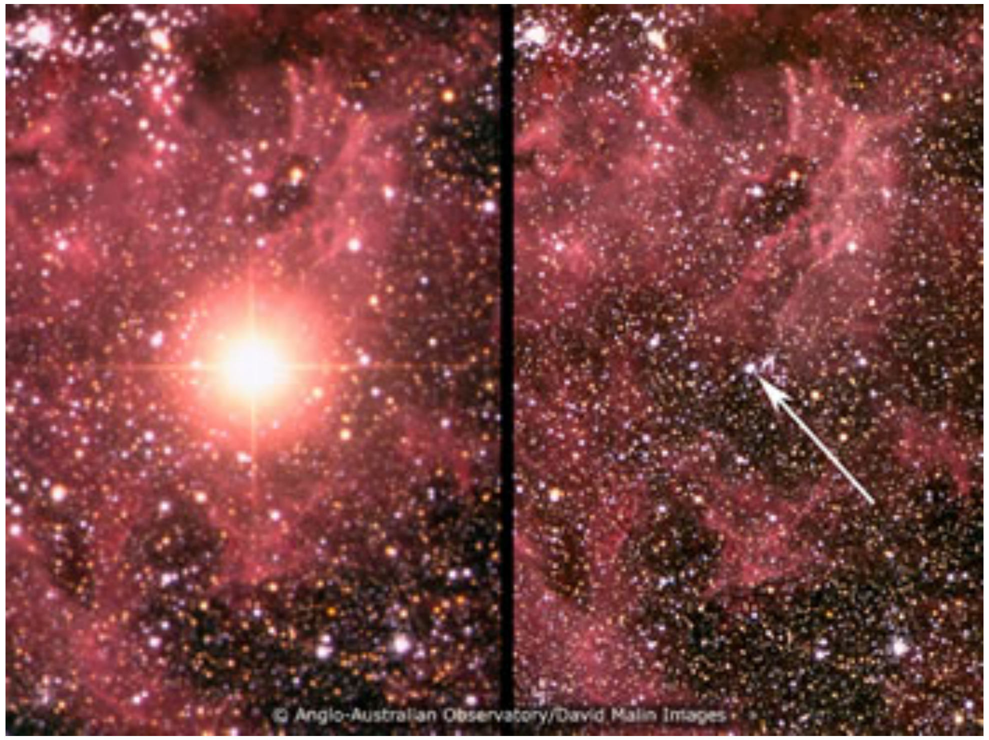

Nearby SN candidates $d_{\rm SN} \lesssim 400$ pc

HIP	Common Name	Distance (pc)
65474	Spica / α Virginis	77(4) [28]
81377	ζ Ophiuchi	112(2) [28]
71860	α Lupi	143(3) [28]
80763	Antares / α Scorpii	169(30) [28]
107315	Enif / ϵ Pegasi	211(6) [28]
27989	Betelgeuse / α Orionis	222^{+48}_{-34} [29]
109492	ζ Cephei	256(6) [30]
24436	Rigel / β Orionis	264(24) [28]
31978	S Monocetotis A(B)	282(40) [28]
25945	CE Tauri / 119 Tauri	326(70) [30]

https://www-sk.icrr.u-tokyo.ac.jp/sk/sk/supernova.html

Collider detectors

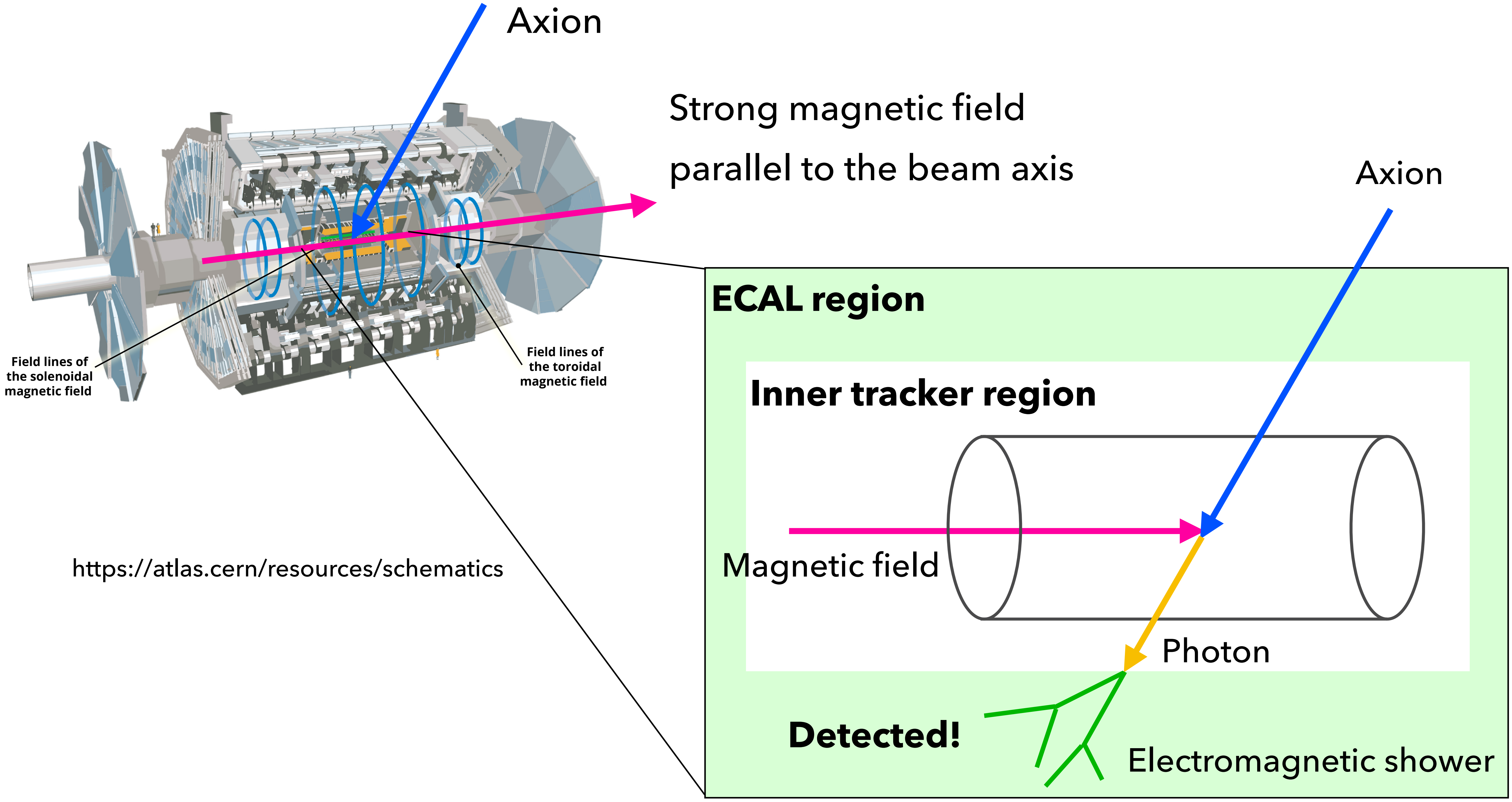

https://atlas.cern/resources/schematics

- Introduction
- Supernova axions
- Axion search with collider detectors
- Summary

Supernova axions

Axion production process

Two kinds of production process occur for $\Delta t_{\mathrm{SN}} \sim 10\ \mathrm{sec}$

- $N_1 + N_2 \to N_1 + N_2 + a$ bremsstrahlung

  $N_i\ (i = 1,\ 2)$ nucleon

P. Carenza, T. Fischer et al., JCAP 10 (2019) 016.

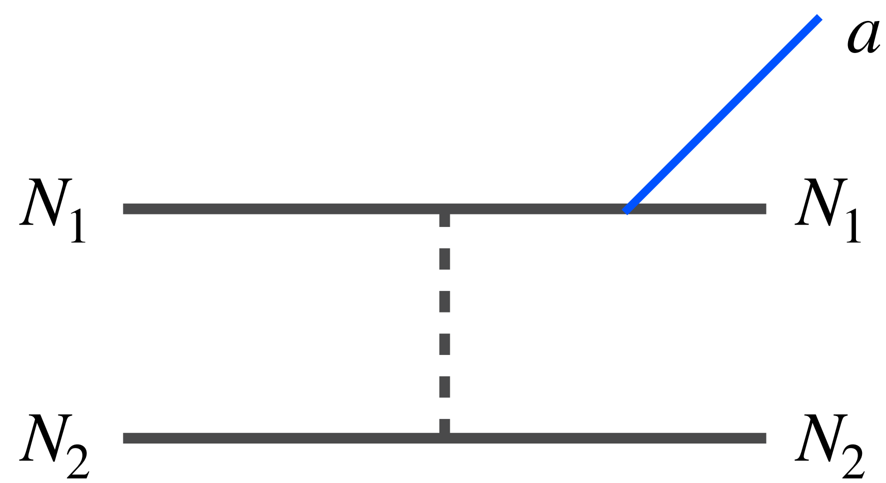

- $\pi^- + p \to n + a$

P. Carenza, B. Fore et al., Phys. Rev. Lett. 126 (2021) 071102.

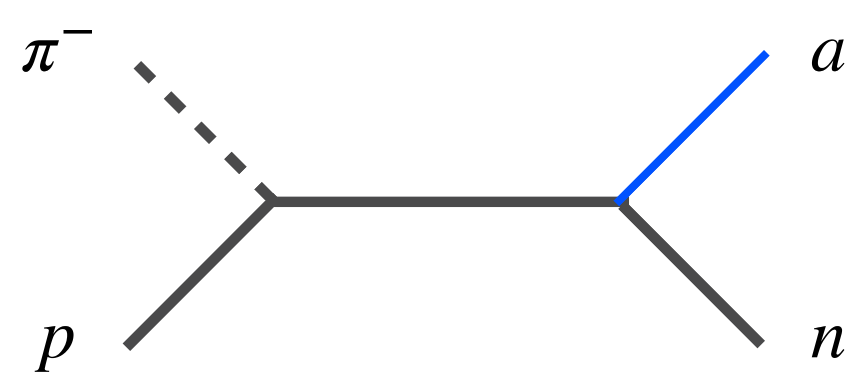

Spectrum

- The peak energy of $\pi^- p$-process axions is roughly three times larger than NN-process ones.
- The spectrum is proportional to $\tilde{g}^2_{aNN}$. $\tilde{g}^2_{aNN} \equiv g^2_{ann} + 0.61 g^2_{app} + 0.53 g_{ann} g_{app}$

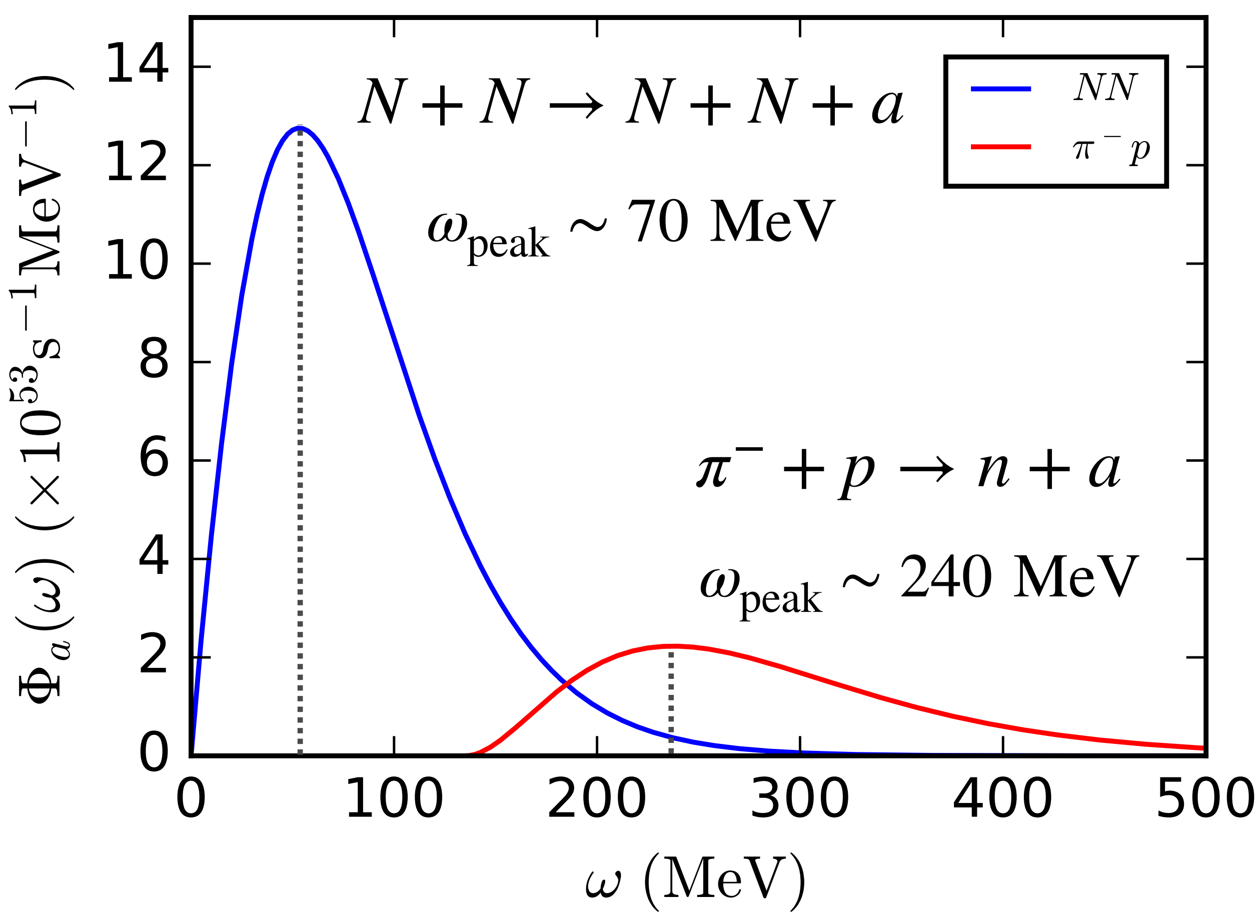

$\tilde{g}_{aNN} = 5 \times 10^{-10}, \kappa_{\rm SN} = 3$

Pre-SN neutrino alert

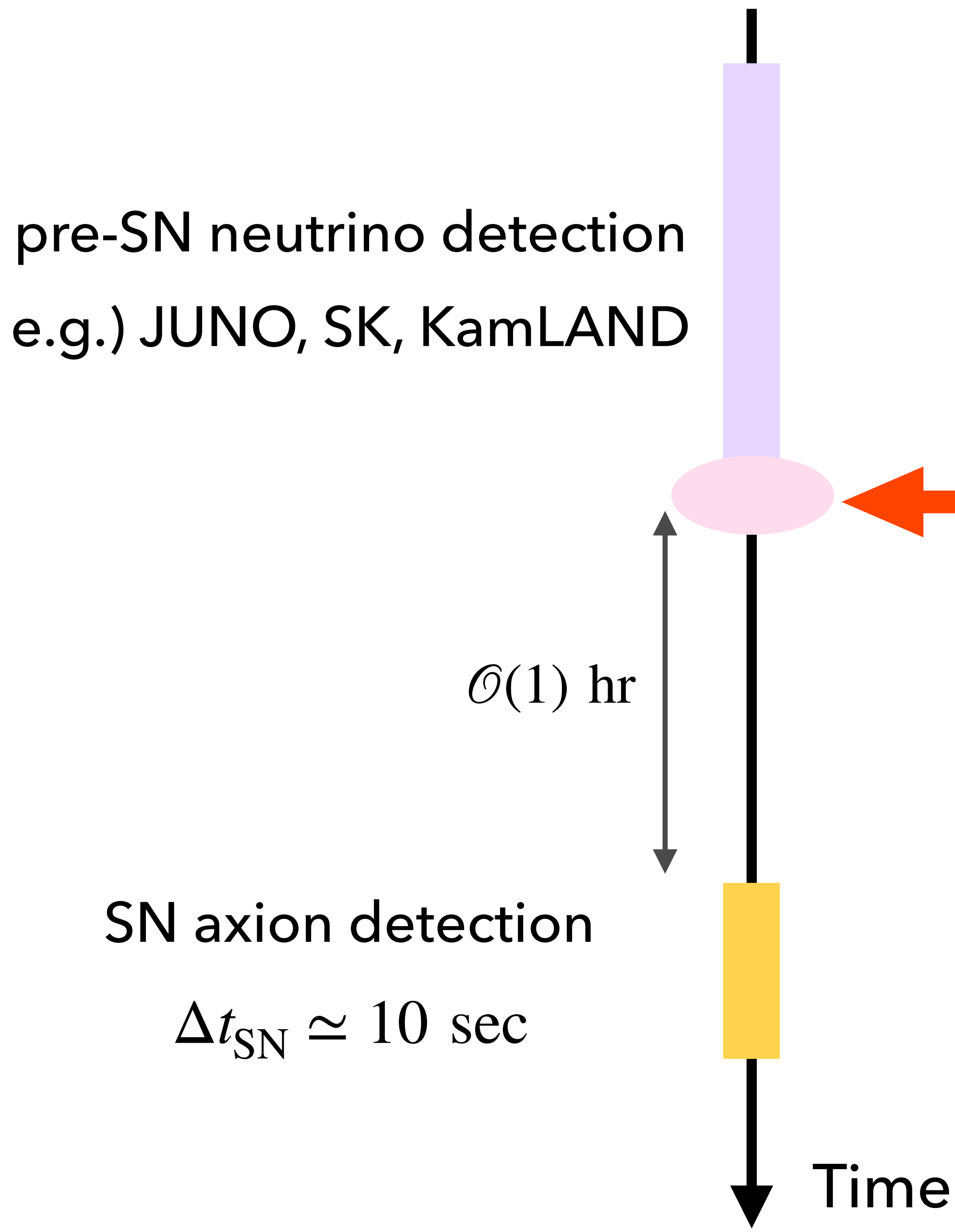

C. Kato, K. Ishidoshiro and T. Yoshida,
Ann. Rev. Nucl. Part. Sci. 70 (2020) 121.

Identify the nearby SN progenitor with the help of pre-SN neutrinos

↓

Stop the beam, and switch to SN axion search

Axion search with collider detectors

Collider detectors

List of detectors

	R	Z	B	$\bar{L}(\theta=\frac{\pi}{6})$	$\bar{L}(\theta=\frac{\pi}{3})$	$\bar{L}(\theta=\frac{\pi}{2})$
ATLAS (LHC) [41]	1.1 m	6.7 m	2.0 T	1.2 m	1.4 m	1.8 m
CMS (LHC) [42]	1.3 m	5.8 m	3.8 T	1.3 m	1.9 m	2.1 m
ILD (ILC) [43]	1.8 m	4.9 m	3.5 T	1.6 m	2.6 m	2.9 m
SiD (ILC) [43]	1.2 m	3.3 m	5.0 T	1.1 m	1.7 m	2.0 m

Inner tracker region

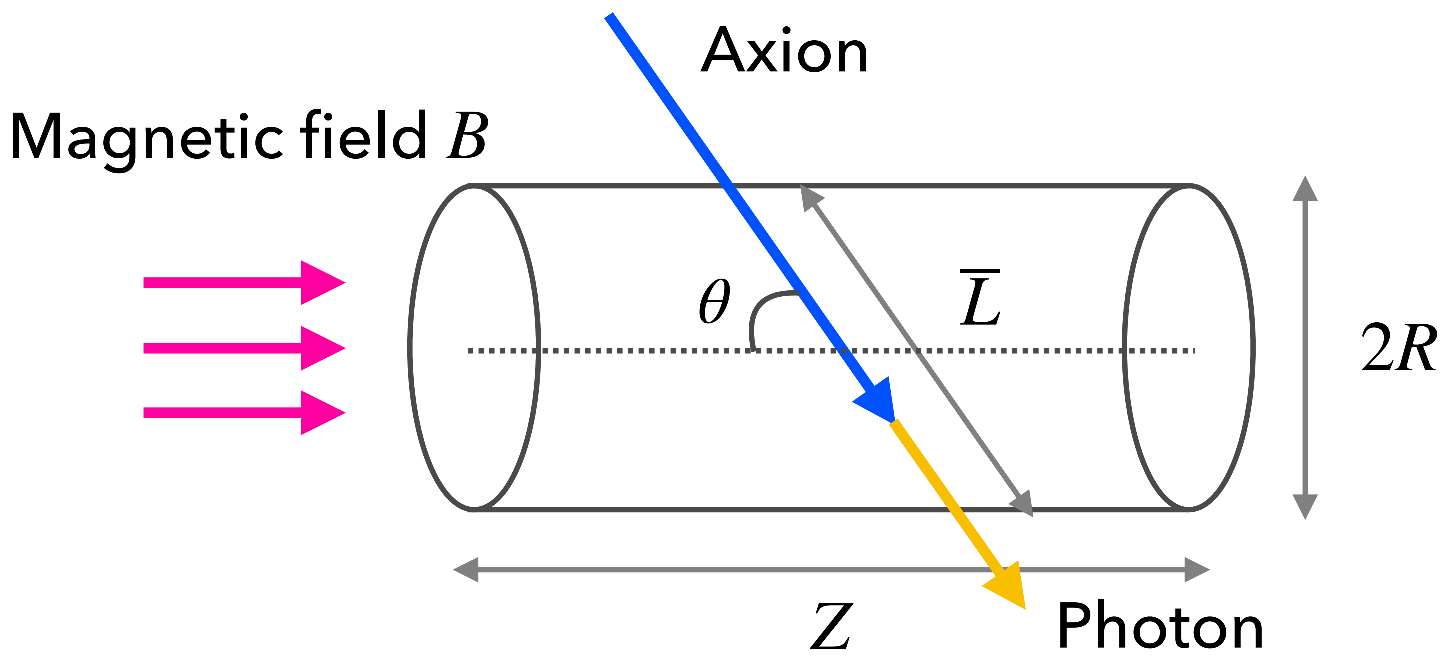

Collider detectors

List of detectors

	R	Z	B	$\bar{L}(\theta=\frac{\pi}{6})$	$\bar{L}(\theta=\frac{\pi}{3})$	$\bar{L}(\theta=\frac{\pi}{2})$
ATLAS (LHC) [41]	1.1 m	6.7 m	2.0 T	1.2 m	1.4 m	1.8 m
CMS (LHC) [42]	1.3 m	5.8 m	3.8 T	1.3 m	1.9 m	2.1 m
ILD (ILC) [43]	1.8 m	4.9 m	3.5 T	1.6 m	2.6 m	2.9 m
SiD (ILC) [43]	1.2 m	3.3 m	5.0 T	1.1 m	1.7 m	2.0 m

Inner tracker region

Conversion rate

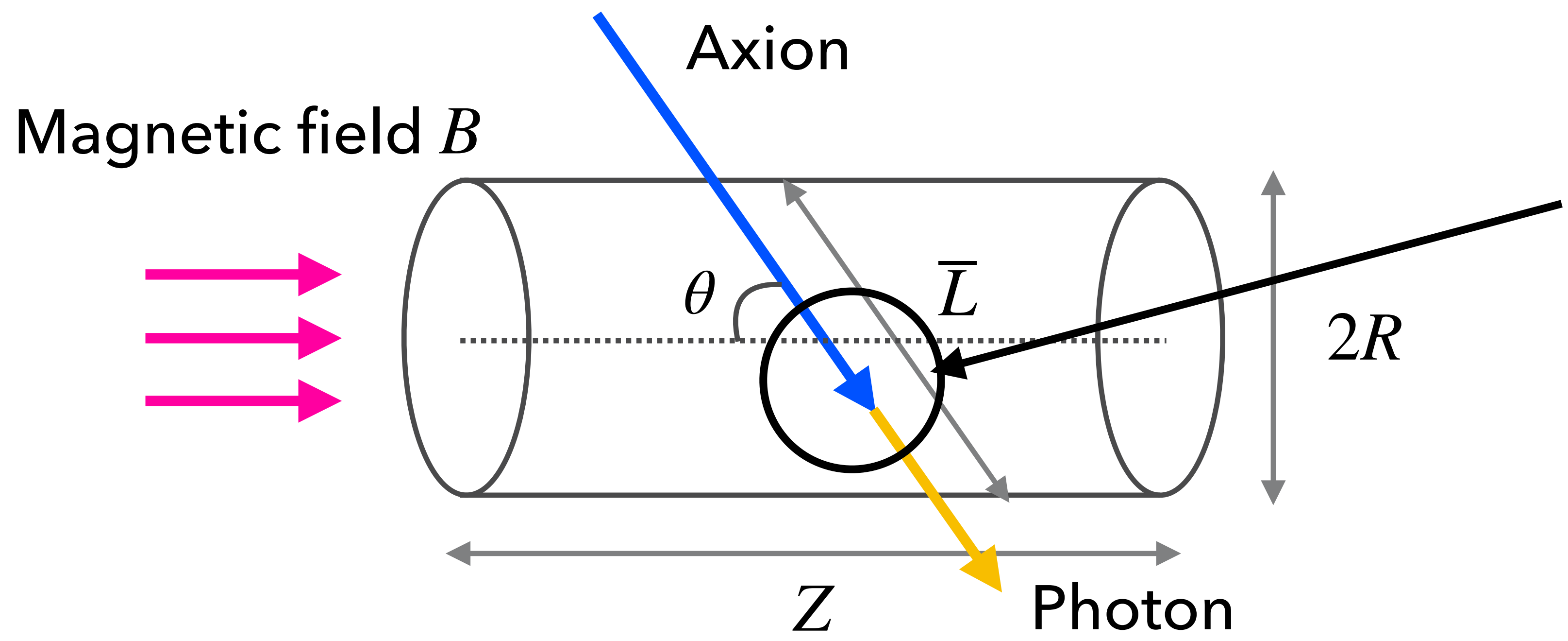

$$P \simeq \frac{1}{4}(g_{a\gamma\gamma} B \bar{L})^2$$

Signal and background

- SN neutrinos interact with materials in ECAL absorber.

$$\nu_e + W \to e^- + X^* \quad \text{(ILD)}$$

Signal and background

- SN neutrinos interact with materials in ECAL absorber.

$$\nu_e + W \to e^- + X^* \quad \text{(ILD)}$$

Background

$N_{BG} \sim 10^5$

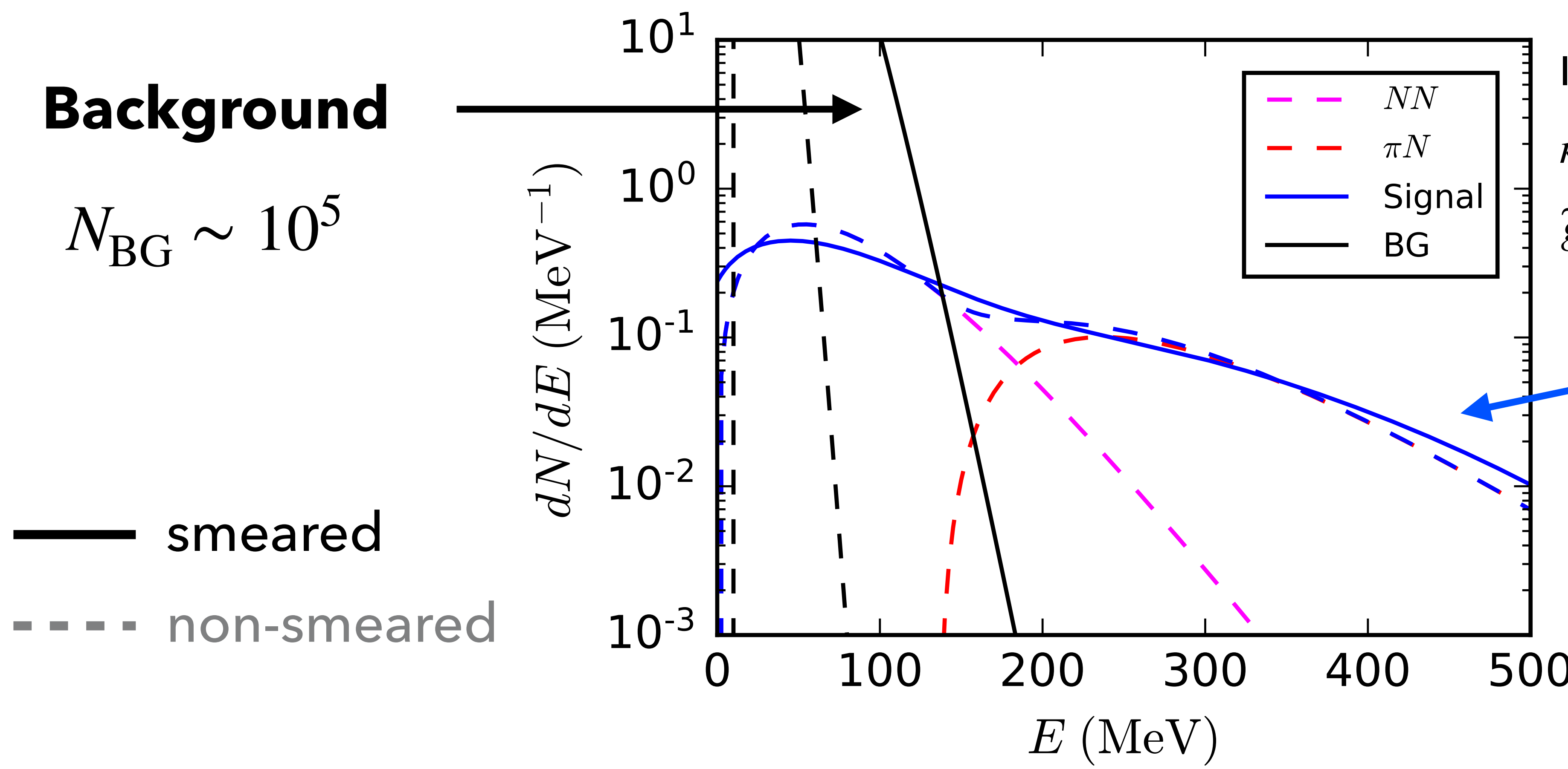

ILD setup, $d_{SN} = 77$ pc (Spica), $\kappa_{SN} = 3$, $g_{a\gamma\gamma} = 6.6 \times 10^{-11}$ GeV^{-1}, $\tilde{g}_{aNN} = 6.4 \times 10^{-10}$, $\Delta t_{SN} = 10$ sec.

Total signal

$N_{signal} \simeq 80$

Signal and background

- We impose an energy cut-off to remove most of background events.

$E_{\rm cut} = 145\ {\rm MeV}$

$N_{\rm BG} \sim 10^5$ ← → $N_{\rm BG} \simeq 1, N_{\rm signal} \simeq 25$

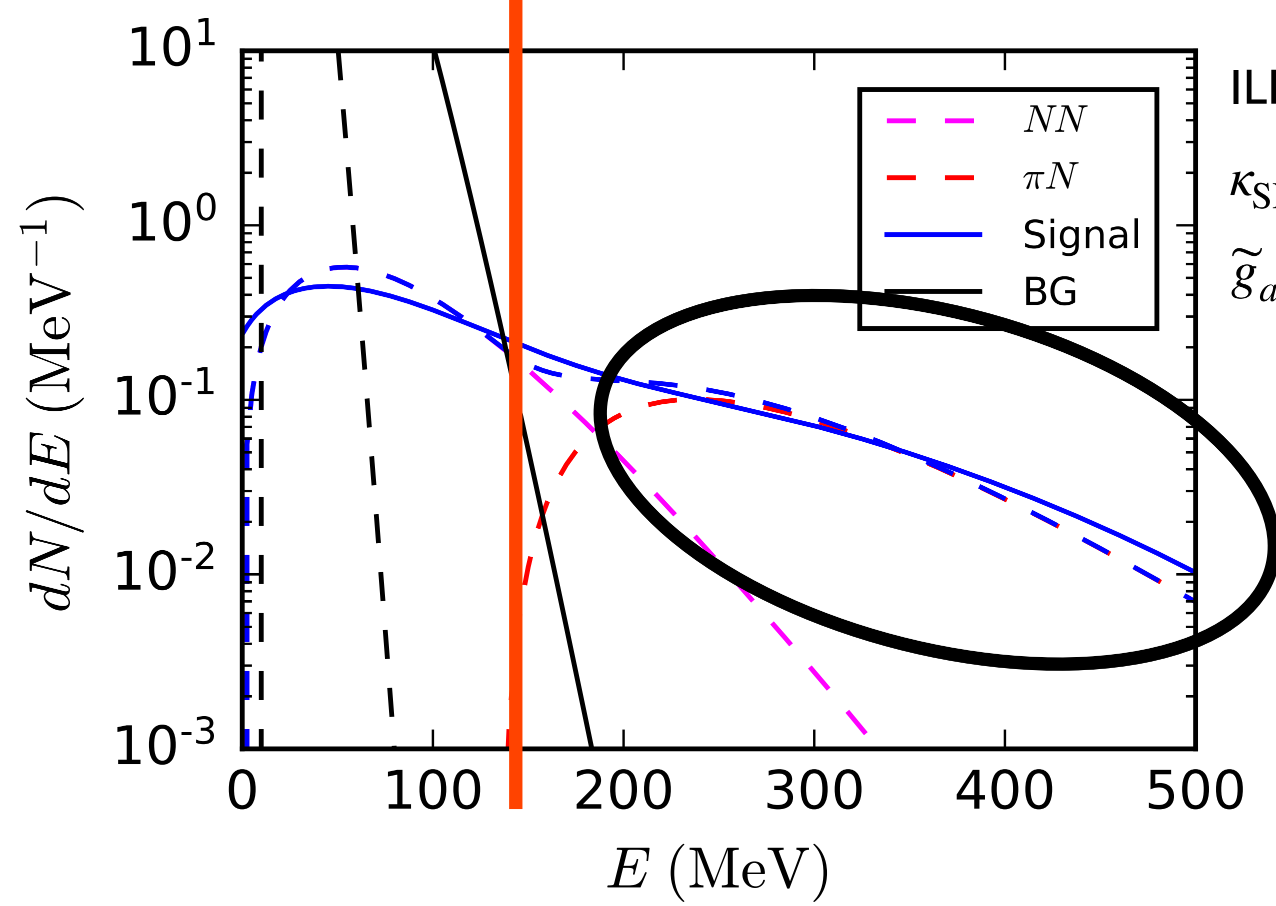

ILD setup, $d_{\rm SN} = 77$ pc (Spica), $\kappa_{\rm SN} = 3$, $g_{a\gamma\gamma} = 6.6 \times 10^{-11}\ {\rm GeV}^{-1}$, $\tilde{g}_{aNN} = 6.4 \times 10^{-10}$, $\Delta t_{\rm SN} = 10$ sec.

Mainly $\pi^- p$-process

smeared

non-smeared

Accessible parameter region

- If a SN occurs within $\mathcal{O}(100)$ pc, we may search unknown region.
- The accessible region can be also searched by IAXO, which is a future solar axion experiment.

ILD setup

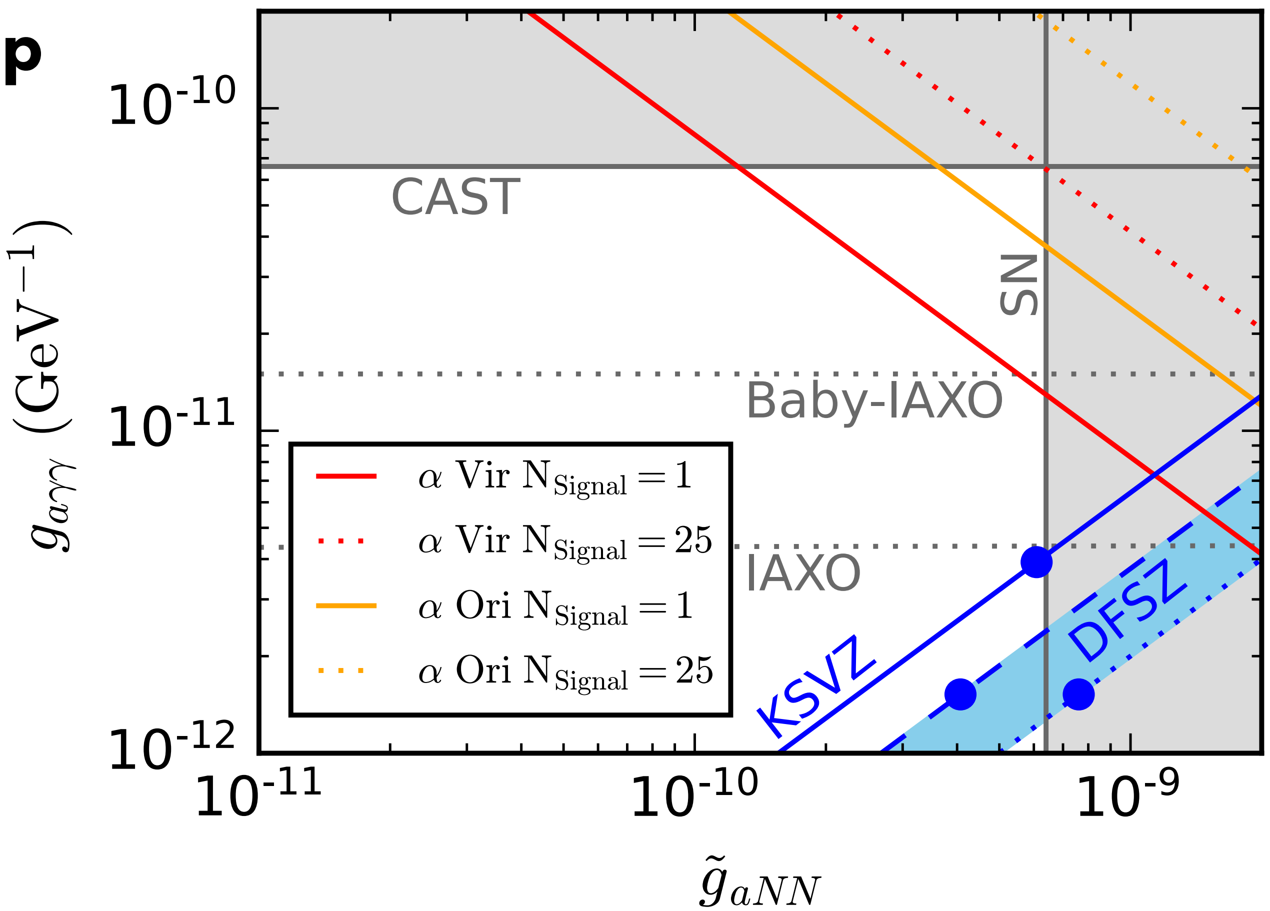

α Vir 77 pc

α Ori 222 pc

Summary

- We have discussed a possibility of SN axion search with collider detectors.
- Practically, we switch to axion search with the help of pre-SN neutrino alert.
- If a nearby SN occurs, we may search non-excluded parameter region.

Supernova + **Collider detector**

→ **New direction to axion search!**

Backup

Production and detection

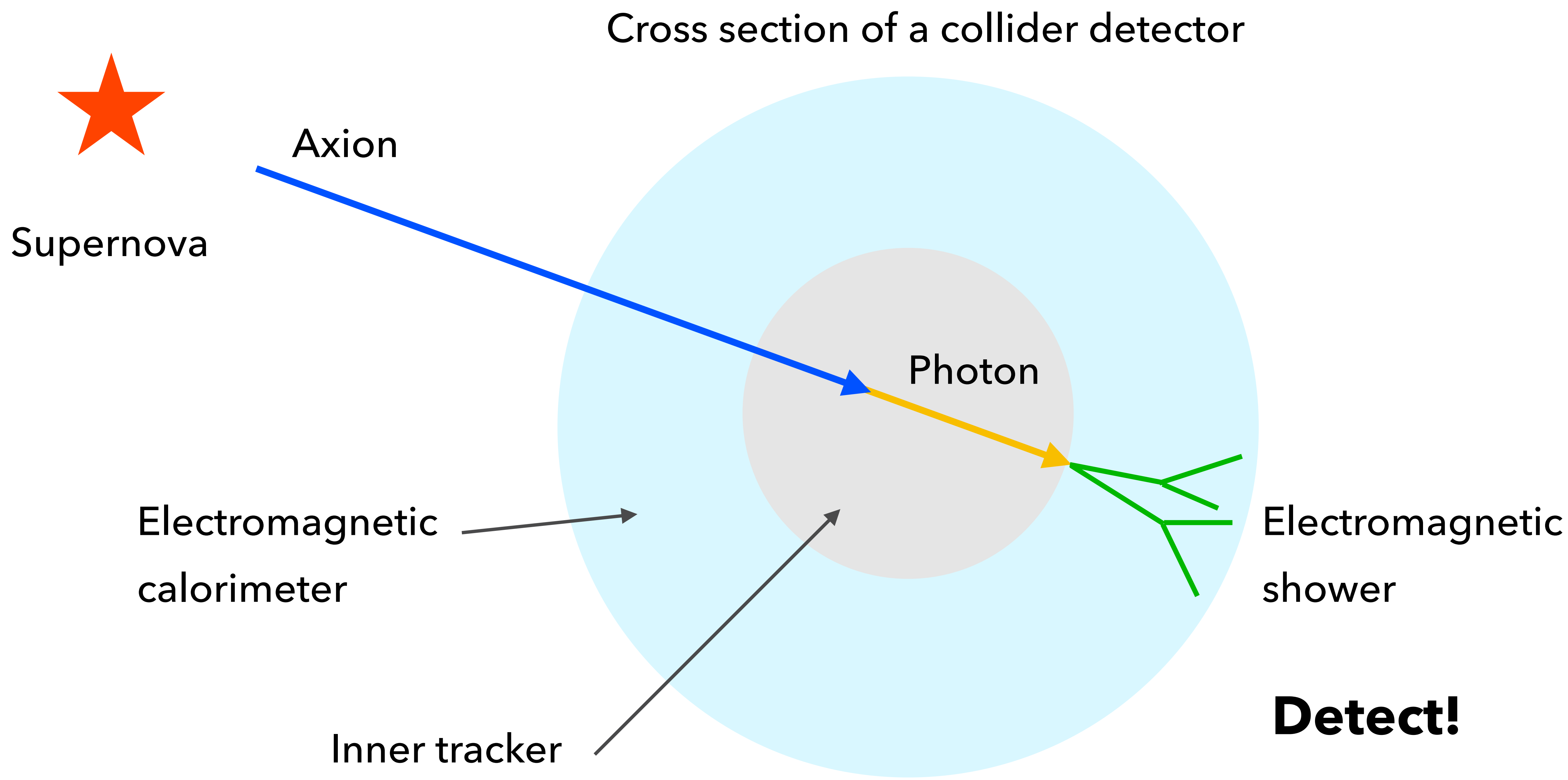

Strong magnetic field $\sim \mathcal{O}(1)$ T

QCD axion

Axion-photon coupling

$$g_{a\gamma\gamma} = \frac{1}{f_a} C_{a\gamma\gamma} \qquad C_{a\gamma\gamma} \simeq \frac{\alpha}{2\pi}\left(\frac{E}{N} - 1.92\right)$$

Axion-nucleon coupling

$$g_{aNN} = \frac{m_N}{f_a} C_{aNN} \quad (N = p, n)$$

$$C_{app}^{\mathrm{(KSVZ)}} \simeq -0.47 \qquad C_{app}^{\mathrm{(DFSZ)}} \simeq -0.617 + 0.435 \sin^2\beta$$

$$C_{ann}^{\mathrm{(KSVZ)}} \simeq -0.02 \qquad C_{ann}^{\mathrm{(DFSZ)}} \simeq 0.254 - 0.414 \sin^2\beta$$

Axion mass

$$m_a \simeq 5.70\ \mathrm{meV} \times \left(\frac{f_a}{10^9\ \mathrm{GeV}}\right)^{-1}$$

G. Grilli Di Cortona, E. Hardy, J. Pardo Vega and G. Villadoro, JHEP **01** (2016) 034.

Constraint on axion-photon coupling

The most stringent bound

$$g_{a\gamma\gamma} \lesssim 0.66 \times 10^{-10}\ \mathrm{GeV}^{-1} \text{ for } m_a \lesssim 0.02\ \mathrm{eV}$$

CAST collaboration, Nature Phys. 13 (2017) 584.

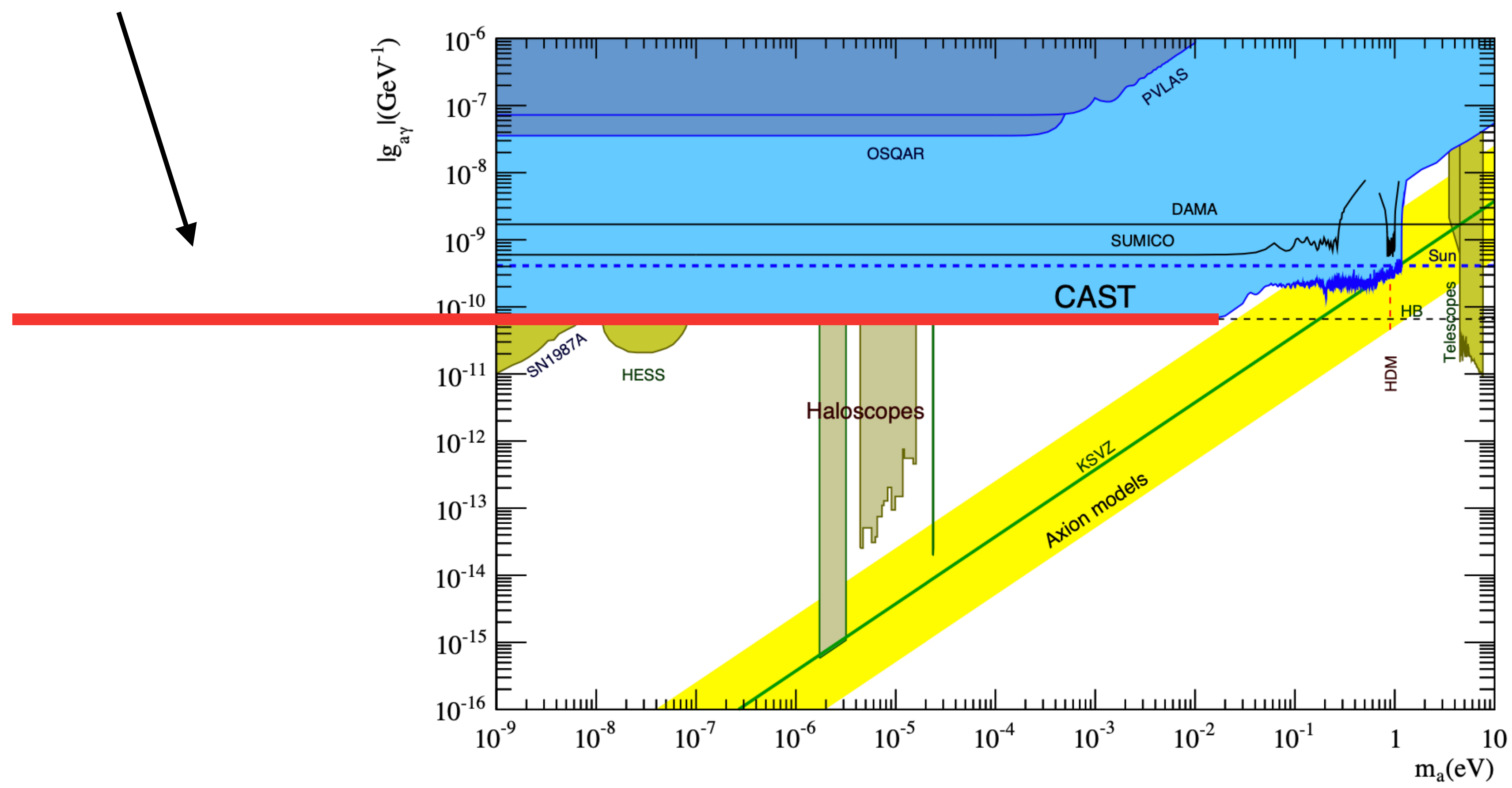

Constraint on axion-nucleon coupling

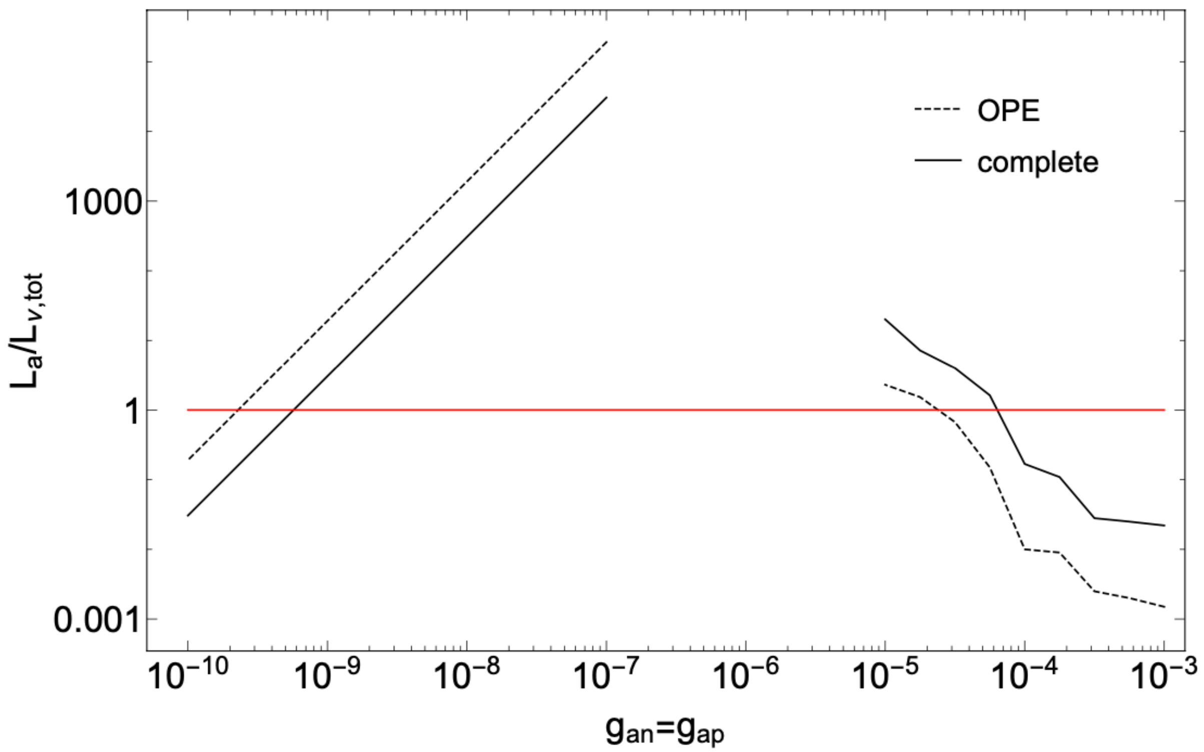

P. Carenza, T. Fischer et al., JCAP 10 (2019) 016.

→ $L_a \lesssim L_\nu \simeq 2 \times 10^{52}$ erg/sec $\quad L_a = L_a^{(NN)} + L_a^{(\pi^- p)}$ (Assuming $L_a^{(NN)} = L_a^{(\pi^- p)}$)

Using $L_a^{(NN)} = 2.42 \times 10^{70}$ erg/sec $\times \tilde{g}_{aNN}^2$

→ $\tilde{g}_{aNN} \lesssim 6.4 \times 10^{-10}$

Pre-SN neutrino alert

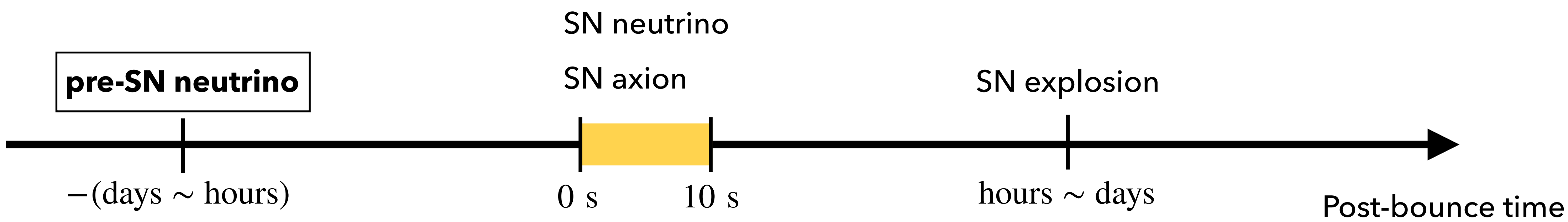

1. Pre-SN neutrinos are emitted $\mathcal{O}(1)$ hour before axion emission.

2. Pre-SN neutrinos are detected by neutrino detectors, e.g.) JUNO, SK, KamLAND.

3. SN candidates within $\mathcal{O}(100)$ pc may be identified $\mathcal{O}(1)$ hour before axions come.

C. Kato, K. Ishidoshiro and T. Yoshida, Ann. Rev. Nucl. Part. Sci. 70 (2020) 121.

4. Stop the beam, and switch to SN axion search.

Alarm time for SN

Table 2 Detection ranges and alarm times for normal (inverted) mass ordering, where a false alarm rate is 1 yr^{-1}, for four pre-SN neutrino models with 15 $M_\odot$.

Detector	Model	$N_s^{DC}(t = 0.01)$	Detection range [pc]	Alarm time [hr]	t_w [hr]
SK-Gd	Kato	46.7–49.9 (10.9–11.7)	380–480 (180–230)	0.1-0.6 (–0.02)	12
		50.8–54.3 (12.2–13.0)	350–460 (170–220)	0.2–4.5 (–0.02)	24
		54.3–58.0 (13.3–14.3)	320–430 (160–210)	0.2–10 (–0.01)	48
	Yoshida	21.4–22.8 (12.4–13.2)	260–330 (190–250)	0.1–1 (–0.1)	12
		26.3–28.0 (15.0–16.0)	260–340 (190–260)	0.4–6 (–0.2)	24
		28.4–30.2 (16.1-17.2)	240–320 (180–240)	0.2–6.5 (–0.2)	48
	Odrzywolek	45.3–48.3 (12.8–13.7)	380–490 (200–260)	4–6.5 (0.02–1.7)	12
		47.3–50.4 (13.4–14.3)	340–460 (180–240)	3–6.5 (–1.6)	24
		49.1-52.4 (14.0-14.9)	310–420 (170–220)	3–7 (–0.7)	48
	Patton	43.5–46.3 (12.9–13.9)	370–480 (200–260)	3.5–6 (0.02–0.9)	12
		45.8–48.9 (13.8–14.7)	340–450 (180–250)	3–6.5 (–0.5)	24
		46.8–49.8 (14.1–15.0)	310–410 (170–220)	2.5–5.5 (–0.1)	48
KamLAND	Kato	7.6 (1.6)	340–410 (150–190)	0.2-1 (NA)	12
		9.3 (2.1)	350–440 (170–210)	5.5–20 (–0.02)	24
		10.9 (2.6)	360–460 (180–220)	17–26 (–0.1)	48
	Yoshida	4.5 (2.4)	260–310 (190–230)	0.5–16 (–0.1)	12
		6.5 (3.5)	290–370 (210–270)	8–18 (0.1–1.8)	24
		7.7 (4.1)	310–390 (220–280)	15–22 (0.3–7.5)	48
	Odrzywolek	9.7 (2.8)	380–460 (200–240)	5.5–8 (0.04–1.7)	12
		11.0 (3.1)	380–480 (200–250)	7–13 (0.08–2)	24
		12.4 (3.5)	390–490 (200–260)	11–38 (0.1–2.5)	48
	Patton	10.1 (2.9)	390–470 (200–250)	5.5–8.5 (0.07–1.9)	12
		11.4 (3.5)	390–490 (210–260)	7–11 (0.1–2.5)	24
		12.2 (3.6)	380–490 (210–260)	7.5–13 (0.1–3)	48
JUNO	Kato	232 (48.7)	950 (430)	54 (24)	12
		286 (65.2)	950 (440)	64 (28)	24
		341 (81.8)	960 (470)	62 (34)	48
	Yoshida	142 (75.7)	740 (540)	52 (30)	12
		205 (109)	810 (590)	64 (38)	24
		247 (131)	810 (590)	62 (46)	48
	Odrzywolek	303 (86.2)	1090 (580)	78 (14)	12
		344 (97.8)	1050 (560)	76 (28)	24
		391 (111)	1030 (540)	74 (48)	48
	Patton	315 (90.6)	1110 (590)	30 (17)	12
		360 (106)	1070 (580)	34 (19)	24
		385 (115)	1020 (550)	38 (20)	48

At the latest $\mathcal{O}(1)$ hr

C. Kato, K. Ishidoshiro and T. Yoshida,

Ann. Rev. Nucl. Part. Sci. 70 (2020) 121.

Our SN model

We use the following SN model by obtaining the spectrum of the NN-process axion.

- Uniform SN
- Proton fraction per baryons $Y_p = 0.3$
- Density $\rho = 1.3 \times 10^{14}\ \mathrm{g/cm^3}$
- Temperature $T = 35\ \mathrm{MeV}$
- KSVZ axion model

Time dependence of the luminosity

We define the time average luminosity, using a parameter, $\kappa_{\rm SN}$.

$$\overline{L}_a^{(NN)} = \kappa_{\rm SN} L_a^{(NN)}(t_{\rm pb} = 1\ {\rm s}) = 2.42 \times 10^{70}\ {\rm erg/sec} \times \tilde{g}_{aNN}^2 \kappa_{\rm SN} \qquad \kappa_{\rm SN} \sim \mathcal{O}(1)$$

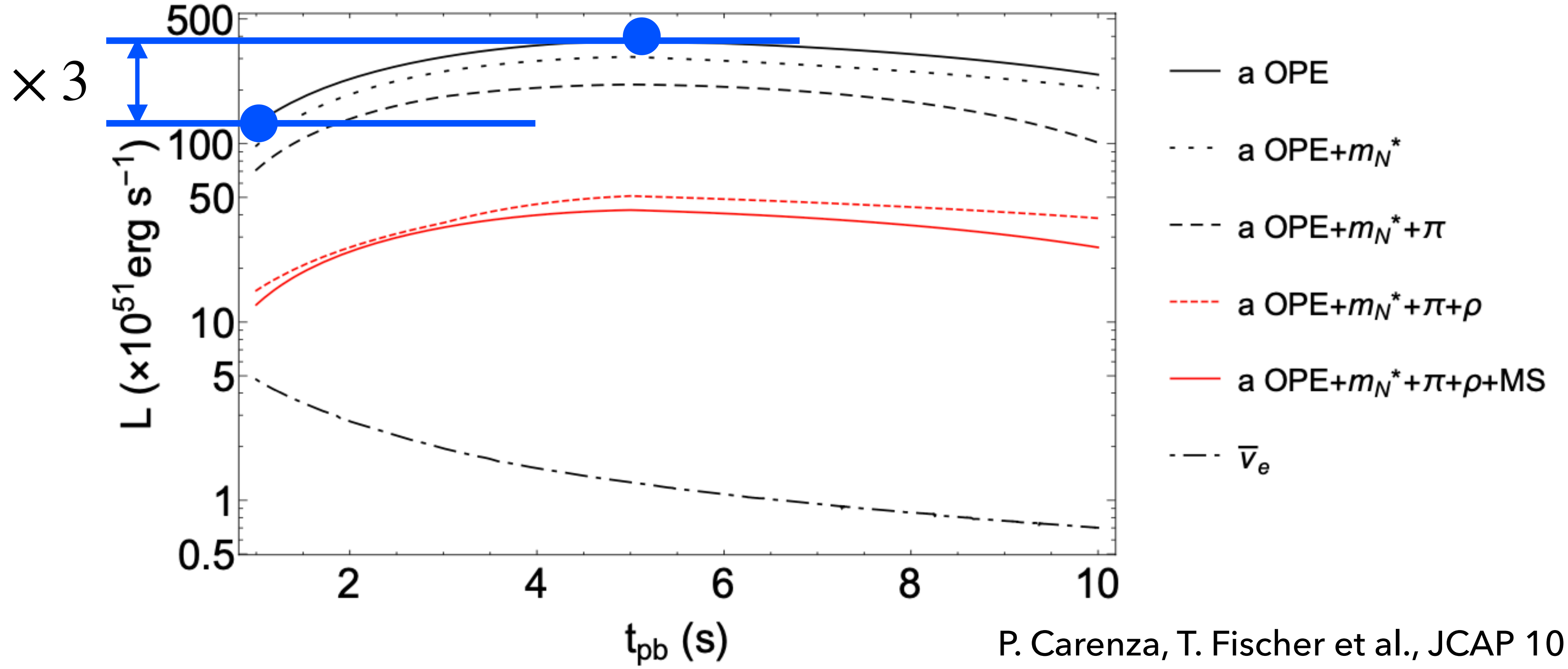

P. Carenza, T. Fischer et al., JCAP 10 (2019) 016.

Spectrum of $\pi^- p$-process axion

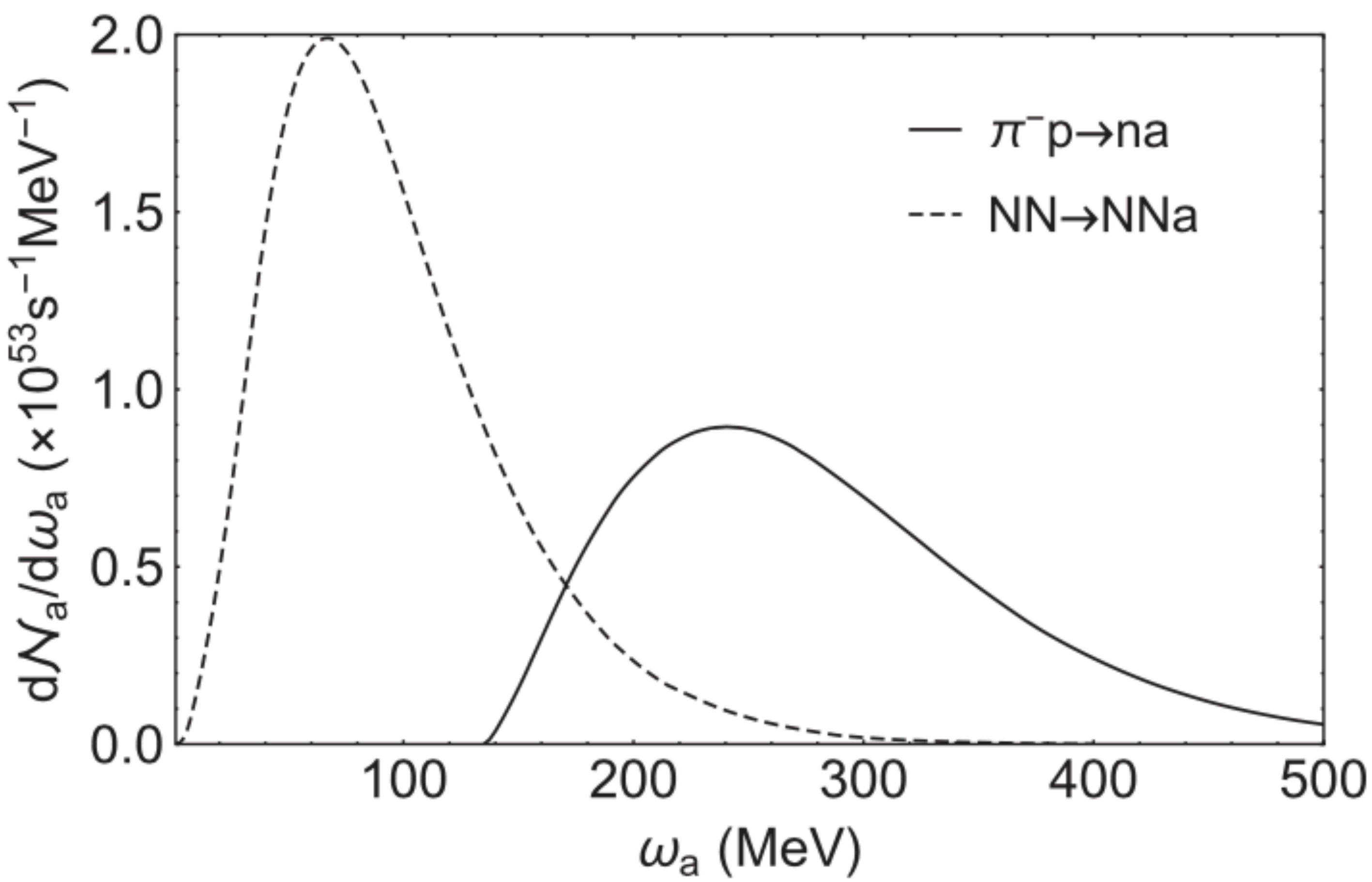

P. Carenza, B. Fore et al., Phys. Rev. Lett. 126 (2021) 071102.

Luminosity

- The luminosity of $\pi^{-}p$-process axion is a few times larger.

NN process $\pi^{-}p$ process

$t_{\rm pb}$ (s)	ρ (10^{14} g/cm^{-3})	T (MeV)	Y_π	Q_a^{NN} (10^{32} erg cm^{-3} s^{-1})	Q_a^{π} (10^{32} erg cm^{-3} s^{-1})	$Q_a^{\rm tot}/Q_a^{NN}$	L_a (10^{51} erg s^{-1})
1	1.45	37.07	0.011	1.37	4.63	4.38	4.0
2	2.08	38.93	0.016	3.28	8.87	3.70	8.10
4	3.10	40.56	0.027	9.08	15.87	2.75	16.63
6	3.65	39.91	0.034	12.92	14.99	2.16	18.61

P. Carenza, B. Fore et al., Phys. Rev. Lett. 126 (2021) 071102.

Conversion rate

Time evolution equation

$$i\partial_L \begin{pmatrix} A_{\|} \\ a \end{pmatrix} = \begin{pmatrix} \omega & g_{a\gamma\gamma}B_T/2 \\ g_{a\gamma\gamma}B_T/2 & \omega - q \end{pmatrix} \begin{pmatrix} A_{\|} \\ a \end{pmatrix},$$

$A_{\|}$:Photon a : Axion

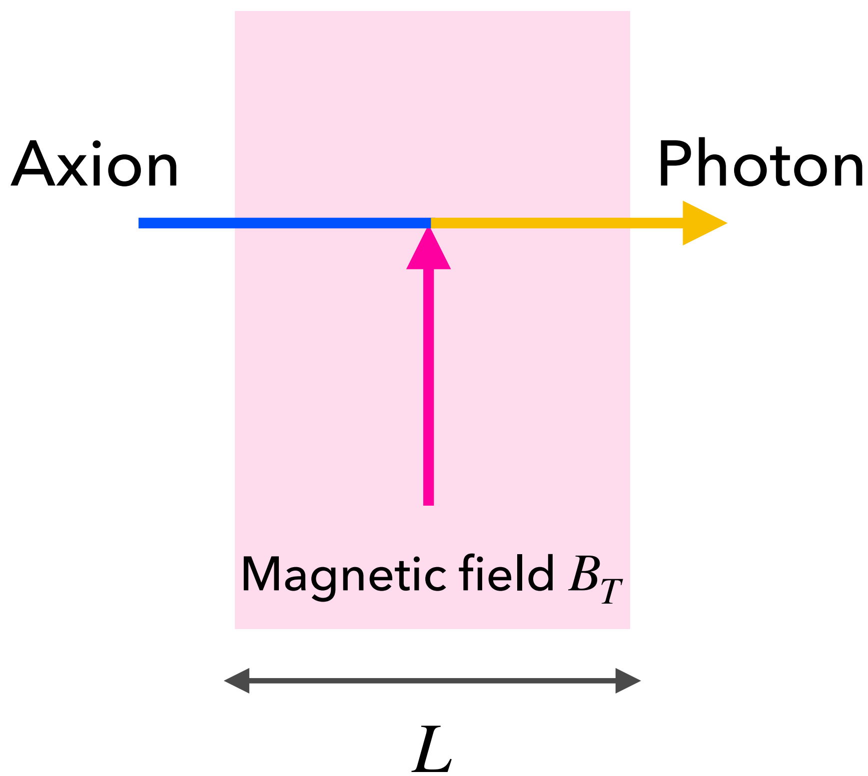

Conversion rate

$$P = \frac{1}{4}(g_{a\gamma\gamma}B_T L)^2 \left(\frac{\sin(qL/2)}{qL/2}\right)^2 \qquad q \equiv \frac{m_a^2}{2\omega}$$

m_a : Axion mass

ω : Axion energy

G. Raffelt and L. Stodolsky, Phys. Rev. D 37 (1988) 1237.

Radiation length (LHC)

- $\sim 1X_0$ → It is difficult to regard a photon as a free particle.

  X_0 : radiation length

ATLAS

C. Gemme,
"The ATLAS Tracker Detector for HL-LHC",
ATL-ITK-PROC-2020-008.

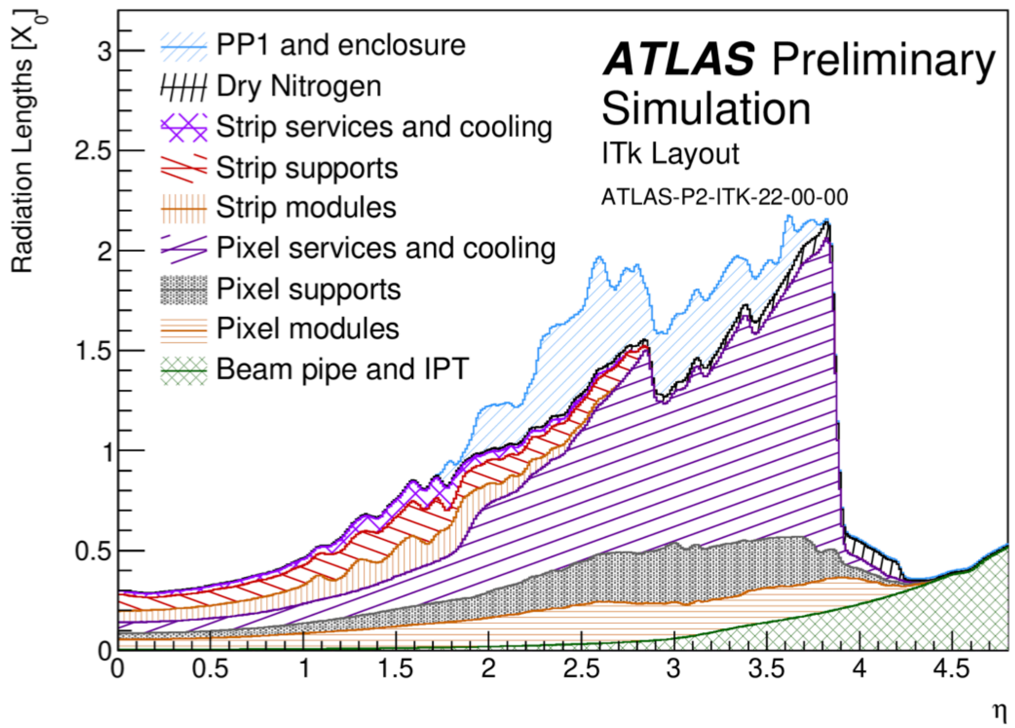

CMS

CMS Tracker collaboration,
"The Upgrade of the CMS Tracker at HL-LHC",
JPS Conf. Proc. 34 (2021) 010006.

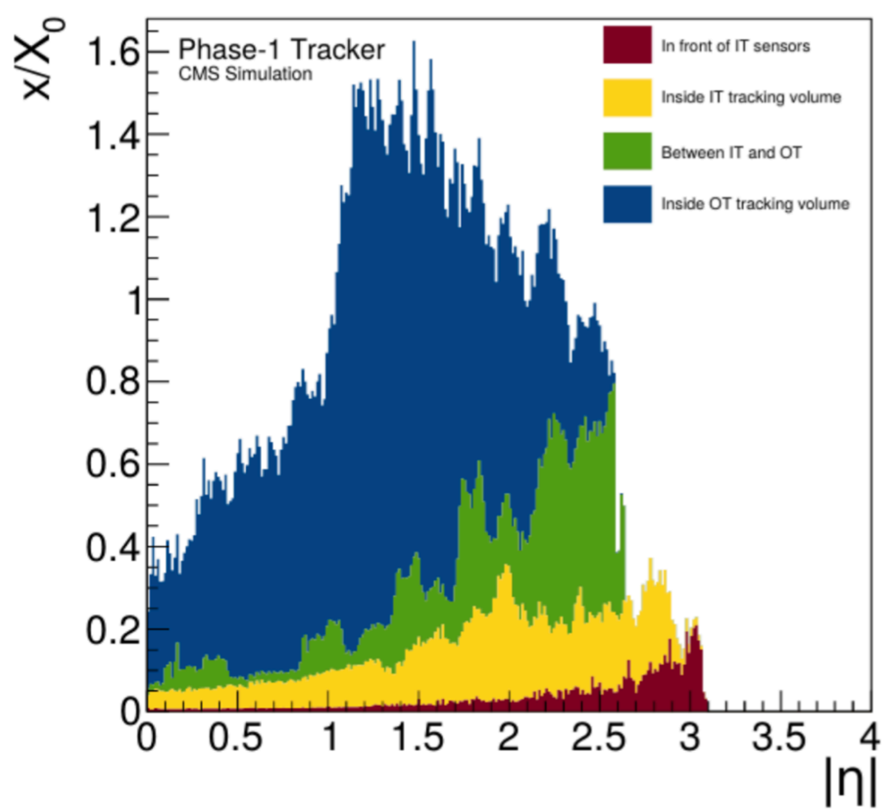

Radiation length (ILC)

- $\sim 0.1 X_0$ → Photon is almost regarded as a free particle.

  X_0 : radiation length

H. Abramowicz et al., 1306.6329.

<u>ILD</u>

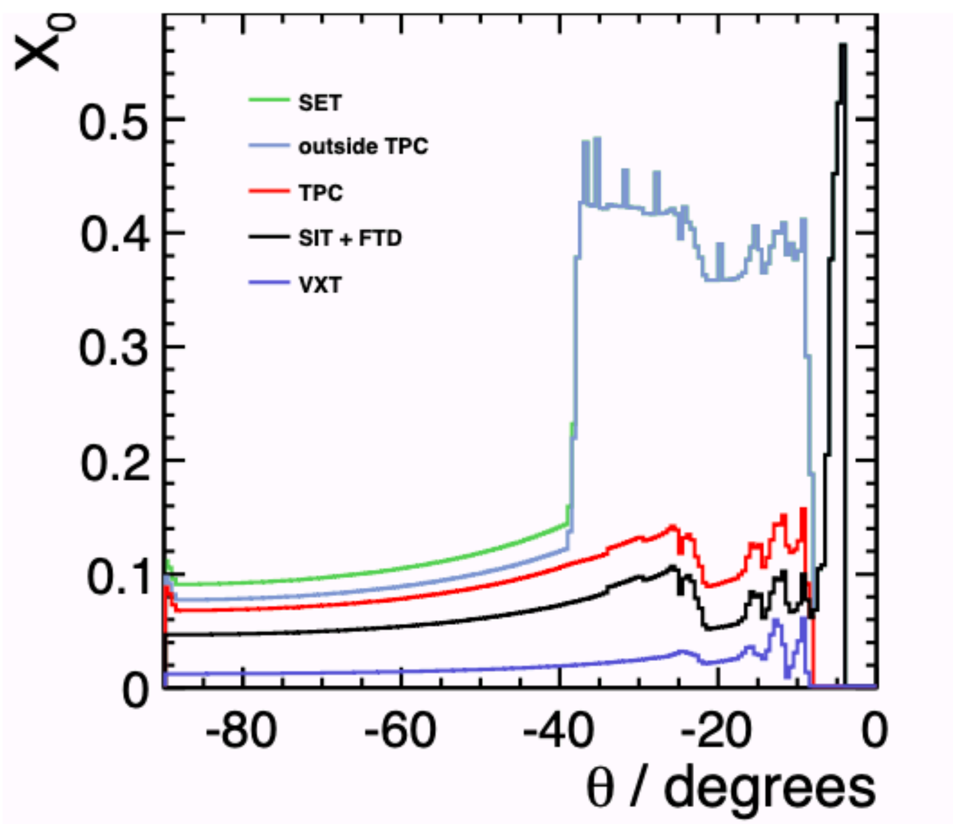

<u>SiD</u> ($\sim 1\,\%\ X_0$/layer)

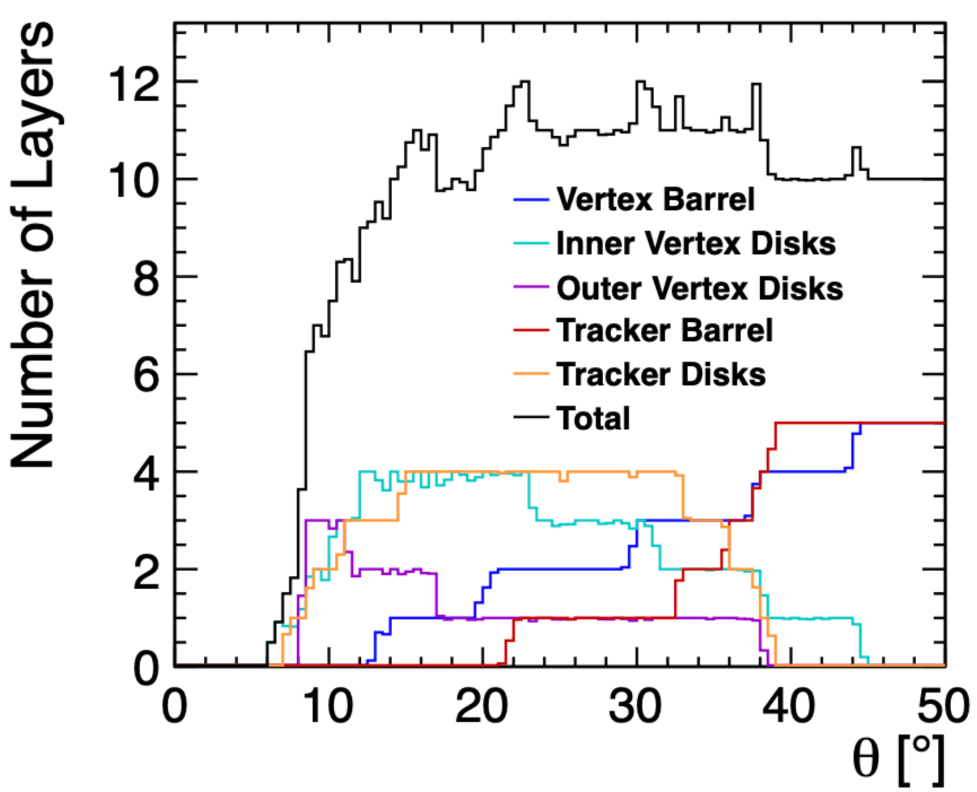

The number of signal events

$N_\gamma =$ (The number of emitted axions per unit time)

× (Emission duration)

× (Ratio of cross sectional area) $= \dfrac{2RZ}{4\pi d_{\rm SN}^2}$

× (Conversion rate)

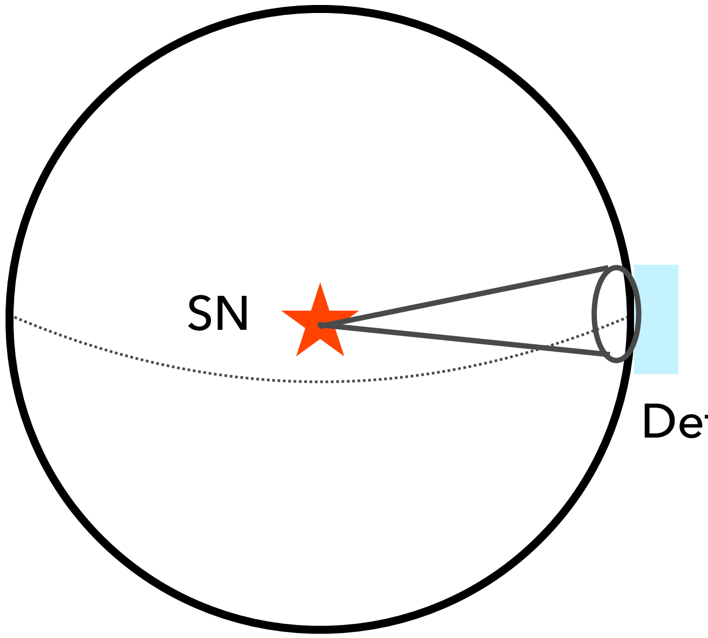

$$N_\gamma \simeq 25 \times \left(\frac{2RZ}{15\ \mathrm{m}^2}\right)\left(\frac{\bar{L}}{2\ \mathrm{m}}\right)^2\left(\frac{B}{4\ \mathrm{T}}\right)^2$$
$$\times \left(\frac{\kappa_{\rm SN}}{3}\right)\left(\frac{d_{\rm SN}}{100\ \mathrm{pc}}\right)^{-2}\left(\frac{\Delta t_{\rm SN}}{10\ \mathrm{sec}}\right)\left(\frac{g_{a\gamma\gamma}}{7\times 10^{-11}\ \mathrm{GeV}^{-1}}\right)^2\left(\frac{\tilde{g}_{aNN}}{6\times 10^{-10}}\right)^2 .$$

Neutrino background events

$$N_{\rm BG} = \Delta t_{\rm SN} N_{\rm target} \int dE_\nu \; f_{\nu_e}(E_\nu)\sigma(E_\nu)$$

$\alpha_e = 2.92$

$\overline{E}_{\nu_e} = 10.01 \text{ MeV}$

$L_{\nu_e} = 4.8 \times 10^{51} \text{ erg/sec}$

at $t = 1991$ ms

Flux

$$f_{\nu_e}(E_\nu) = \frac{L_{\nu_e}}{4\pi d_{\rm SN}^2 \overline{E}_{\nu_e}^2} \frac{(\alpha_e + 1)^{\alpha_e + 1}}{\Gamma(\alpha_e + 1)} \left(\frac{E_\nu}{\overline{E}_{\nu_e}}\right)^{\alpha_e} e^{-(\alpha_e+1)E_\nu/\overline{E}_{\nu_e}}$$

Scattering cross section $\sigma(E_\nu) \sim 10^{-39} - 10^{-41} \text{ cm}^2$ for $E_\nu \sim 10$ MeV

(For $\nu_e + \mathrm{Pb} \to e^- + \mathrm{Bi}^*$ case)

Tamborra, B. Muller, L. Hudepohl, H.-T. Janka and G. Raffelt, Phys. Rev. D 86 (2012) 125031.

The number of targets $N_{\rm target} \sim 4 \times 10^{29}$ for ILD (tungsten)

H. Abramowicz et al., 1306.6329.

$\to N_{\rm BG} \sim 10^5$

$\Delta t_{\rm SN} \simeq 10$ sec, $d_{\rm SN} \sim 100$ pc

The energy cut-off and signal events

- The number of signal events with $E_{\rm cut} = 150$ MeV is roughly one-third of the one without the energy cut-off.

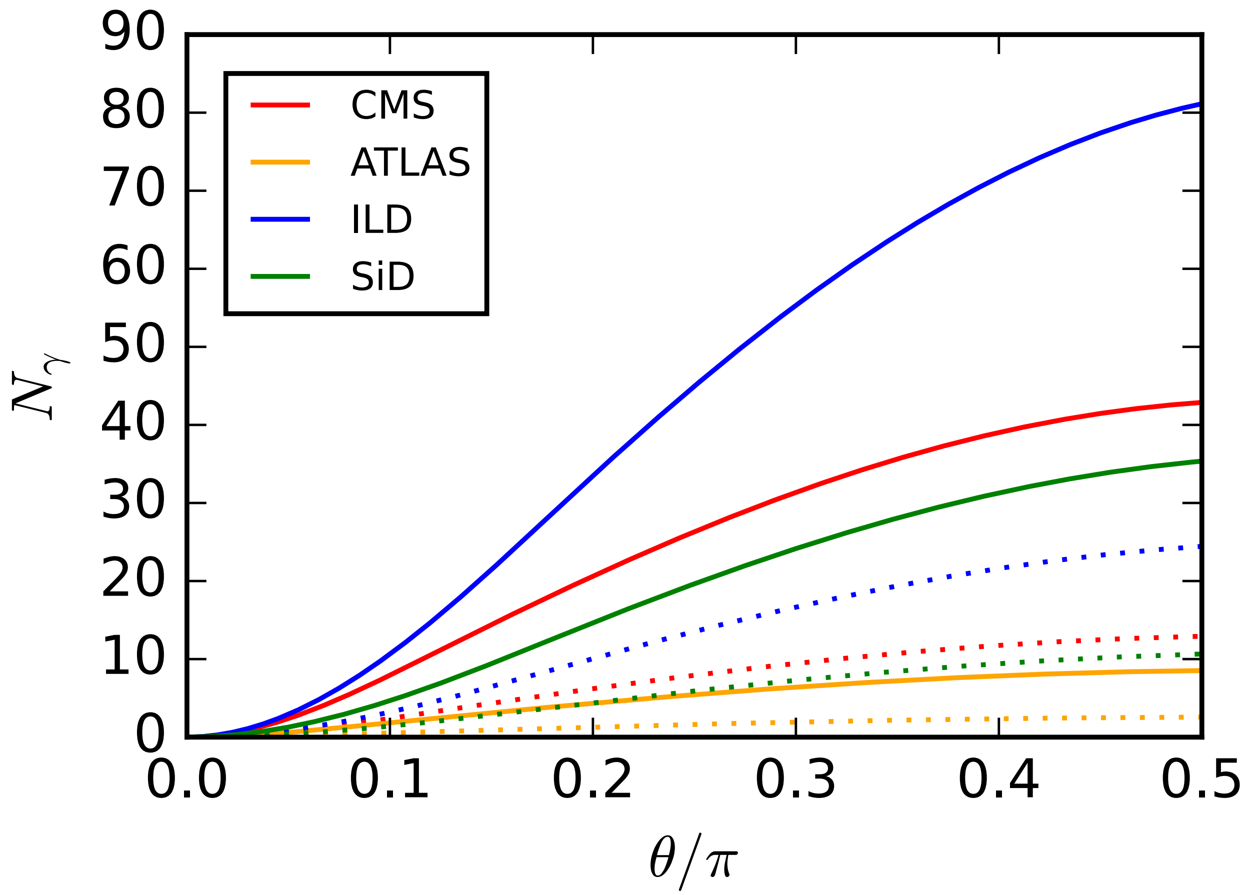

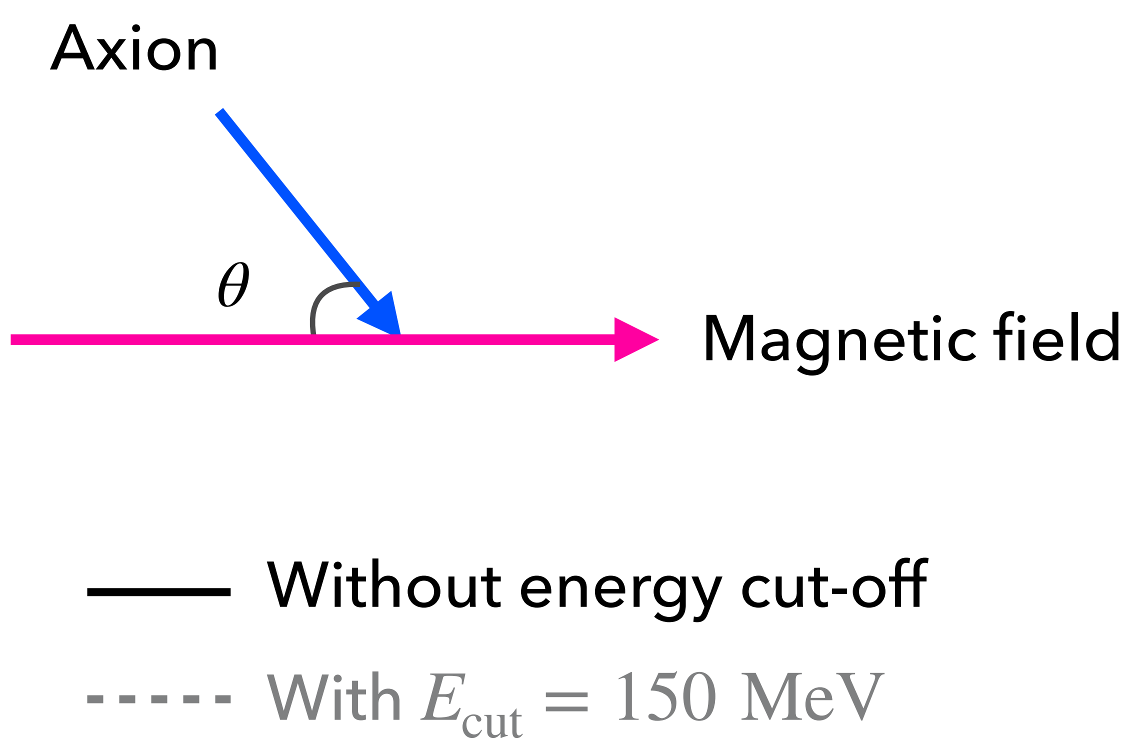

Energy resolution

- Practically, the energy resolution is finite.
- We regard quantities smeared by the Gaussian function as observables.

$$f^{(\mathrm{obs})}(E) = \int dE' \frac{1}{\sqrt{2\pi}\delta E} \exp\left(-\frac{(E'-E)^2}{2\delta E^2}\right) f^{(\mathrm{ori})}(E')$$

$$\frac{\delta E}{E} = \frac{a}{\sqrt{E_{\mathrm{GeV}}}}$$

$a = 15\,\%$ for ILD (W)

H. Abramowicz et al., 1306.6329.

$a = 17\,\%$ for SiD (W)

$$E_{\mathrm{GeV}} \equiv \frac{E}{1\ \mathrm{GeV}}$$

$a = 3\,\%$ for CMS (PbWO4)

CMS collaboration, JINST 8 (2013) P09009.

Energy resolution and signal events

ILD setup

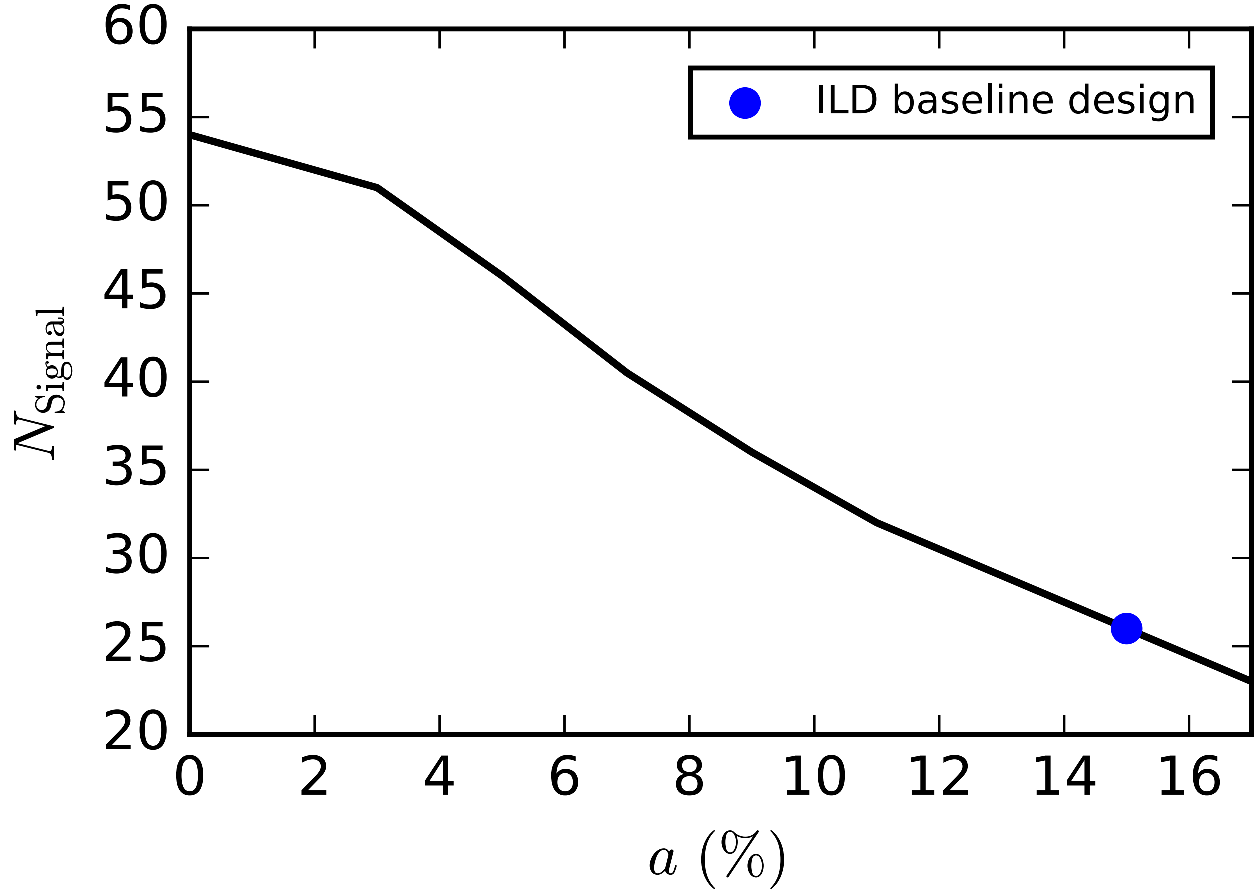

$$\frac{\delta E}{E} = \frac{a}{\sqrt{E_{\text{GeV}}}}$$